energies

MDPI

Article

Comparison Study on Photo-Thermal Energy Conversion Performance of Functionalized and Non-Functionalized MWCNT Nanofluid

Tsogtbilegt Boldoo [1], Jeonggyun Ham [2] and Honghyun Cho [2,*]

1 Department of Mechanical Engineering, Graduate school of Chosun University, 309 Pilmundaero, Dong-gu, Gwangju 61452, Korea; tsogtbilegt31@gmail.com

2 Department of Mechanical Engineering, Chosun University, 309 Pilmundaero, Dong-gu, Gwangju 61452, Korea; orchiders@chosun.kr

* Correspondence: hhcho@chosun.ac.kr

Received: 17 August 2019; Accepted: 29 September 2019; Published: 1 October 2019

check for updates

Abstract: Multiwalled carbon nanotubes (MWCNTs) have attracted attention from researchers because of their superior thermal properties and high optical absorption. In this investigation, the thermal and optical properties of functionalized and nonfunctionalized MWCNT nanofluid based on ethylene glycol/water were experimentally studied and compared. The results indicated that the use of the functionalized MWCNT nanofluid improved the thermal properties and optical absorption performance compared with the nonfunctionalized MWCNT nanofluid. The thermal conductivity enhancement of the functionalized MWCNT nanofluid was higher than that of the nonfunctionalized MWCNT nanofluid. The maximum thermal conductivity enhancement (10.15%) was observed in a functionalized MWCNT concentration of 0.01 wt% at 50 °C compared with the base fluid. In addition, the photo-thermal energy conversion efficiency of the functionalized MWCNT nanofluid was higher than that of the nonfunctionalized one owing to its higher light absorption and thermal conductivity.

Keywords: MWCNT (multiwalled carbon nanotubes); functionalized; thermal conductivity; optical transmittance; extinction coefficient

1. Introduction

In recent decades, the emission of greenhouse gases such as CO_2, NO_x and SO_x has been excessive because of the continuous and rapid growth of world energy consumption [1]. Consequently, researchers and manufacturers have studied innovative ways to improve the efficiency of heat exchange devices such as refrigerator, air conditioning, industrial heat transfer equipment and power plant. The best way to reach the high heat transfer efficiency that contributes to higher performance and eco-friendly properties in heat exchange equipment is to enhance the favorable properties of working fluid in the thermal system. For this reason, Choi et al. [2] introduced the novel idea of using nanofluid, which suspends nanosized materials with high thermal properties such as metal, metallic oxides and carbon nanotubes, into the base fluid.

The thermal conductivity of nanofluid can be enhanced by increasing the intensity of Brownian motion that is dominant mechanism and can be more activated by rising temperature [3–9]. Accordingly, using the proper nanoparticles in various nanofluid is a fundamental research topic to achieve a highly efficient working fluid. Nanofluid can also considerably augment the capability of photo-thermal energy conversion and optical scattering of working fluids. Among the working fluids, water is an almost perfect working fluid, however, the good thermal properties of water can be reduced when antifreeze is added to the water owing to unfavorable operating conditions.

To develop a highly efficient solar thermal collector system, many nanofluids have been used as a working fluid in various types of solar thermal collectors such as a direct absorption solar collector (DASC), flat-plate, evacuated tube and dish type and so forth. Furthermore, the optical properties of nanofluid should be improved to increase the efficiency of solar collectors and especially, to develop a highly efficient DASC. Kang et al. [10] studied the flat-plate and U-tube solar collectors using Al_2O_3 nanofluid and they reported that the electrical consumption reduction of flat-plate and U-tube solar collector was 1546.56 kWh and 1315.9 kWh, respectively, because of efficiency improvement by using Al_2O_3 nanofluid. Furthermore, the electrical cost saving a year by using the flat-plate and U-tube solar collector with nanofluid was 510.4 and 432 USD in Germany. Lee et al. [11] used Al_2O_3 and CuO nanofluid in the PVT system (Photo-voltaic thermal system) and their experimental results indicated that the CuO and Al_2O_3 based PVT systems exhibited higher efficiency than water-based PVT system because of thermal conductivity improvement in the working fluid. Sarafraz et al. [12] observed that thermal and electrical production of the PVT system improved by 130% and 20% in case of using MWCNT nanofluid instead of water.

Table 1 [13] shows the thermal properties of representative nanoparticles. Among the various nanoparticles, MWCNT probably has the highest thermal conductivity. Moreover, the specific heat of MWCNT is higher than that of other nanoparticles except for Al. In a study by Gan et al. [14], compared with Al and carbon nanoparticles (CNPs), MWCNT nanofluid has a low transmission in the ultraviolet range but higher transmission in the visible range. In addition, MWCNT nanofluid showed an effective optical performance compared with other nanofluid using Al and CNP nanoparticles. Meng et al. [15] reported that MWCNT nanofluid based on ethylene glycol exhibited high thermal conductivity and photo-thermal energy conversion efficiency. In a comparative study by Zeiny et al. [16], MWCNT nanofluid was the most suitable candidate in the DASC compared with gold and copper nanofluid.

Table 1. Thermal properties of representative nanoparticles.

Properties	MWCNT	Ag	Al	Au	Cu	Fe
Thermal conductivity (W/m°C)	3000	406	205	314	385	79.5
Density (kg/m^3)	2100	10510	2707	19300	8954	7897
Specific heat (J/g·°C)	0.72	0.23	0.896	0.13	0.38	0.452

Generally, nanofluid are manufactured by one-step or two-step methods. In the one-step method, nanofluid can be manufactured by using several complicated chemical processes. In the case of the two-step method, nanoparticles are prepared by a form of powder through physical or chemical methods and then they are blended into a base fluid. Kumar et al. [17] reported in the comprehensive study that most researchers commonly used a two-step method than a one-step method in nanofluid manufacturing because the one-step method requires more complicated processes and expensive reagents. However, according to Sidik et al. [18], the one-step method is suitable for small-scale production although a two-step method was less expensive for mass production.

Because of the earth's gravitation and electrical force, there is sedimentation of nanoparticles in the nanofluid, which can have a negative influence on the thermal and optical properties of the nanofluid. In the application of MWCNT nanofluid in thermal systems, the agglomerated particles can cause blockage of the pump and other mechanisms. This dispersion stability problem can be solved by chemical and physical treatments. The chemical treatment is relatively effective to make reliable nanofluid because it increases the interaction force between nanoparticles and base fluid molecules via atomic bonding in nanoscale. The chemical treatment consists of covalent and non-covalent functionalization treatments. In non-covalent functionalization treatment, adding surfactants such as gum-arabic (GA), sodium dodecyl sulfate (SDS) disperse into nanofluid does not change the structure of nanoparticles. On the other hand, the covalent functionalization treatment modifies the structure of nanoparticles by using strong chemical reactions such as adding aqueous acids solutions and oxidizing agents. In the covalent functionalization treatment, using carboxyl acid (-COOH) functionalization group shows good results to guarantee dispersion stability of nanofluid. Barnali et al. [19] used the carboxyl acid (-COOH) functionalization group to stabilize Au nanoparticles and they found that cavitands carrying -COOH groups could stabilize nanoparticles in the working fluid. Yazid et al. [20] conducted a review study of the effect of preparation on the stability of MWCNT nanofluid. In their study, among stabilization methods, the most effective method to stabilize a nanofluid was shown to be the covalent functionalization method, which is effective in the long-term stability of nanofluid. Farbod et al. [21] carried out a stability experiment on MWCNT nanofluid that was functionalized by the covalent method. In their result, no sedimentation was observed in MWCNT nanofluid after 80 days. Further, Karami et al. [22] showed that an alkaline functionalized water-based MWCNT nanofluid yielded significant enhancement of dispersion stability in a low-temperature range.

In the case of high-temperature applications, MWCNT nanofluid had better stability at more than 250 °C after it was stabilized by KPS-functionalization and acid-functionalization compared to the single-walled CNT and double-walled CNT nanofluid [23]. In a study by Hewakuruppu et al. [24], a highly stable nanofluid, such as functionalized MWCNT nanofluid, had nearly identical properties as an ideal working fluid in the DASC. Furthermore, a diluted water-based MWCNT nanofluid showed higher thermal conductivity than ethylene glycol based one because of the high viscosity of ethylene glycol [25]. In addition, the temperature effect on the thermal conductivity enhancement was more noticeable at a higher concentration range in MWCNT nanofluid [26]. Jian et al. [27] reported that the photo-thermal energy conversion potential of MWCNT nanofluid mostly depended on the concentration and the maximum receiver thermal efficiency increased up to 96.4% at the MWCNT mass fraction of 0.01 wt%, which was about 32.5% higher than that of DI water. Besides, they presented that CNT nanoparticles agglomeration was occurred by temperature rising under high mass fractions. Moreover, Zeng et al. [28] studied the thermal performance of MWCNT-SiO_2/Ag nanofluid and they reported the absorption spectrum fitted with the solar spectrum could absorb solar light in all wavelengths because of the low light transmittance of MWCNT nanofluid. Furthermore, Nadooshan et al. [29] reported that MWCNT could be an excellent hybrid magnetic nanofluid with Fe_3O_4.

Most previous studies focused on the influence of nanofluid concentration to enhance the photo-thermal energy conversion properties of MWCNT nanofluid. However, studies on the relation between dispersion stability of nanofluid with thermal properties and efficiency of photo-thermal energy conversion of MWCNT nanofluid have not carried out sufficiently. In addition, the use of functionalized MWCNT nanofluid in the solar thermal collector as a working fluid have not been carried out actively. Moreover, comparative studies on the thermal and optical performances of functionalized and nonfunctionalized MWCNT nanofluid have not been reported in open literature even though two kinds of MWCNT nanofluid are currently used and studied. Due to lack of information on thermal properties and optical properties in related to the photo-thermal energy conversion performance of MWCNT nanofluid, the comparison study on the thermal conductivity and optical transmittance between functionalized and nonfunctionalized MWCNT nanofluid by using -COOH functionalization group were investigated experimentally. Furthermore, comparative results on the enhancement of photo-thermal energy conversion characteristics between functionalized and nonfunctionalized MWCNT nanofluid based on ethylene glycol/water are presented. Generally, the ethylene glycol solution has been used widely because the freezing temperature of the water is not too low, thus it cannot be used in cold climate regions during winter season. The freezing temperature of ethylene glycol/water (20/80) is −7.8 °C [13], thus it is suitable for use during winter season in South Korea. Besides, the addition of ethylene glycol in the water increased the boiling temperature of base fluid, which is 102.2 °C [13], thus this can prevent phase change of working fluid in the high-temperature region.

2. Experimental Setup and Methods

2.1. MWCNT Nanofluid

Manufacturing nanofluid is more complicated than just making a liquid–solid mixture because of their dispersion stability and durable suspension for long-term use in engineering applications. In this experiment, functionalized and nonfunctionalized MWCNT nanofluid was manufactured by a two-step method, which mixes nanoparticles and ethylene glycol/water (base fluid). According to previous studies, there are two ways to make a stable MWCNT nanofluid: one is to add the surfactant and the other is the functionalization of MWCNT nanoparticles. The first method is easier to make a nanofluid because it just adds the surfactant into a nanofluid, which does not change the structure of the nanoparticles. In this study, two manufacturing methods were used to prepare the MWCNT nanofluid for the comparative study. To make the nonfunctionalized MWCNT nanofluid by using the first method, the gum-arabic was used as a surfactant, whereas the functionalized MWCNT nanofluid used MWCNT-COOH to make nanofluid by the second method. Due to the carboxyl group (-COOH) that changes the structure of MWCNT nanoparticles, the functionalized MWCNT nanofluid has better bonding strength and dispersion characteristics.

Moreover, MWCNT nanoparticles functionalized by the COOH method are easily dissolved in base fluid. There was no need to insert the surfactant in the functionalized MWCNT nanofluid, which means a negative effect was not observed during the experiment. The physical properties of MWCNT nanoparticles are shown in Table 2 [30].

Table 2. Physical properties of MWCNT nanoparticles [30].

Item	Specification
Purity	>95%
Color	Black
Outer diameter	10–20 nm
Inner diameter	5–10 nm
Length	10–30 µm
Thermal conductivity	1500–3000 W/m°C
True density	2100 kg/m^3
Manufacturing method	CVD
Content of -COOH	2.00 wt%

To obtain good dispersion stability in nanofluid, the functionalized and nonfunctionalized MWCNTs were dispersed into a 20% ethylene glycol/water solution with weight concentrations of 0.001, 0.002, 0.005 and 0.01 wt% by using an ultrasonic machine for 2 h at 20,000 Hz. The weight concentration of nanofluid can be expressed as Equation (1).

$$wt\% = \frac{w_{np}}{w_{bf} + w_{np}} \cdot 100 \tag{1}$$

where, w_{np} and w_{bf} are the weights of the nanoparticle and base fluid, respectively. Figure 1 shows the picture of functionalized and nonfunctionalized MWCNT nanofluid at different concentrations. According to Figure 1, samples get darker as the concentration of MWCNT nanofluid increases. At all concentrations, nanofluids have good dispersion stability and have no deposition for two months. In addition, the zeta potentials of MWCNT nanofluid was measured and it ranged from −44 to −68 mV for functionalized nanofluid and from −32 to −56 mV for nonfunctionalized MWCNT nanofluid, respectively.

Figure 1. Pictures of 0.001, 0.002, 0.005 and 0.01 wt% functionalized and nonfunctionalized MWCNT nanofluid.

The size and structure of functionalized and nonfunctionalized MWCNT nanoparticles used to make nanofluids were analyzed by the transmission electron microscopy (TEM) image and it is presented in Figure 2. It can be seen that both MWCNT nanoparticles are partially tangled but dispersed consistently. The inner and outer diameters of both functionalized and nonfunctionalized MWCNT nanoparticles are about 5–15 nm and 10–25 nm, which are well in agreement with the specifications of the manufacturer. In addition, it shows that the functionalized MWCNT nanoparticles are comparably straighter and smoother than nonfunctionalized MWCNT nanoparticles.

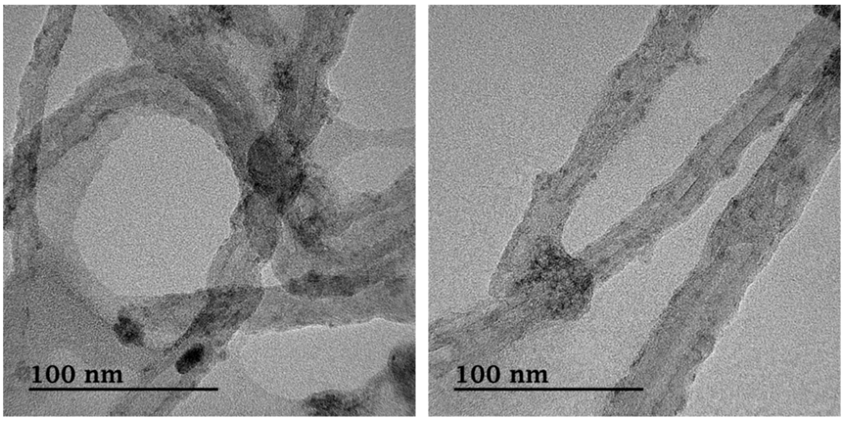

(**a**) Nonfunctionalized MWCNT (**b**) Functionalized MWCNT

Figure 2. Transmission electron microscope (TEM) image of (**a**) nonfunctionalized and (**b**) functionalized multiwalled carbon nanotube (MWCNT) nanofluid with aspect ratio of 100 nm.

2.2. *Thermal Conductivity of MWCNT Nanofluid*

To measure the thermal conductivity of MWCNT nanofluid, KD2-Pro (Decagon Devices, Inc., USA) was used. This device uses a transient hot-wire method, which is based on the measurement of the temperature increment in a defined distance from the linear heat source (hot wire) embedded in the test sample. The heating wire and the temperature sensor were encapsulated in a probe. The thermal conductivity of the nanofluid can be expressed by Equation (2) [31].

$$k = \frac{q(\ln t_1 - \ln t_2)}{4\pi(\Delta T_2 - \Delta T_1)} \tag{2}$$

where, q is the constant heat rate applied to an infinitely long and small "line" source and ΔT_2 and ΔT_1 are the changes in the temperature at t_1 and t_2. The sensor of KD2-Pro was KS-1 vertically inserted into a sample nanofluid, which located in double jacket chamber that connected to the thermal constant bath to control the constant temperature during measuring of thermal conductivity of nanofluid. The sensor probe, which was made of stainless steel with a length of 60 mm and diameter of 1.3 mm, can measure thermal conductivity in the ranges of 0.02 to 2.00 W/m°C. Thermal conductivity was recorded three times at 20-min intervals. Before the measurements of the samples, the measurement device was verified by using ethylene glycol and it showed a good agreement to the reference within error of ±2.3% [32]. Thermal conductivities of 0.001, 0.002, 0.005 and 0.01 wt% MWCNT nanofluid were measured at temperatures ranging from 20 °C to 50 °C. A schematic of the thermal conductivity experimental setup is shown in Figure 3. The experimental setup consisted of the heat exchanger glass beaker, thermal isolator chamber, thermal constant circulation water bath and temperature and thermal conductivity sensors. In addition, the physical properties of the base fluid (20% ethylene glycol/water) with the temperature are shown in Table 3 [32].

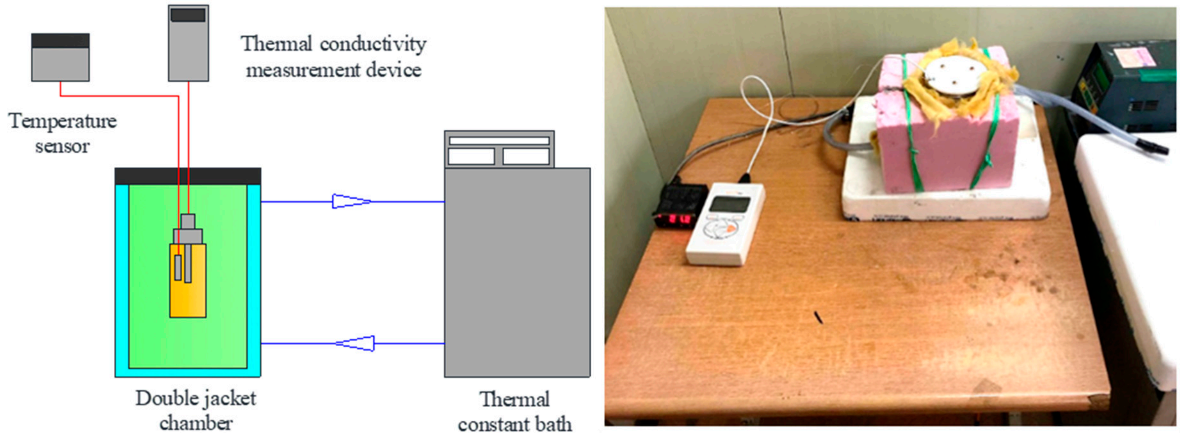

Figure 3. Schematics and picture of thermal conductivity experimental setup.

Table 3. Physical properties of water/ethylene glycol (20 vol%) as a base fluid [32].

Temperature (°C)	Density (kg/m^3)	Viscosity (m^2/s)	Thermal Conductivity (W/m°C)
20	1029.72	1.65	0.497
30	1026.02	1.3	0.509
40	1021.83	1.06	0.52
50	1017.16	0.88	0.529

2.3. Optical Absorption of MWCNT Nanofluid

Among the optical properties, the transmittance and extinction coefficients are critical properties. To investigate the light transmittance spectrum of the MWCNT nanofluid, an optical experiment was carried out at room temperature (25 °C) and wavelengths of light ranging from 300 to 1300 nm. Figure 4 shows the schematic of the optical transmittance experimental setup. The optical transmittance was measured at least three times in a 10-mm glass cuvette to obtain the precise properties. The light from the light source (Avalight-DHc, Apeldoorn Gelderland, Netherlands) passed through the nanofluid and the spectrometer (AvaSpec-ULS2048XL, Apeldoorn Gelderland, Netherlands) measured the light waves.

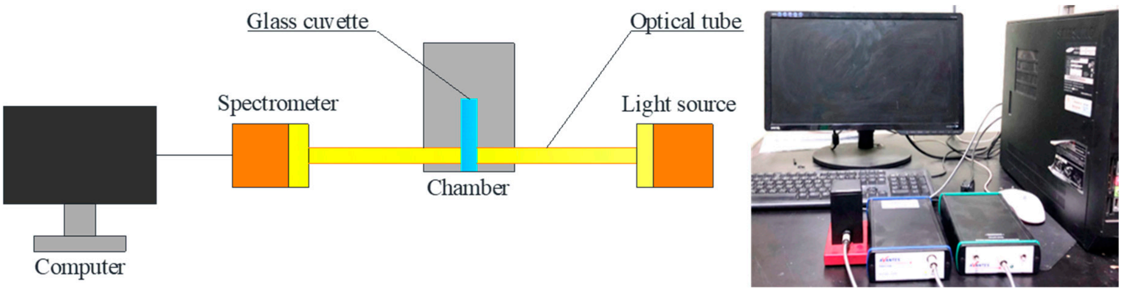

Figure 4. Schematics and picture of optical transmittance experimental setup.

The extinction coefficient is calculated by the Beer–Lambert law [33], which can be expressed by Equation (3).

$$T(\lambda) = \mathrm{e}^{-k(\lambda)_{e,\lambda} y} \tag{3}$$

where, $T(\lambda)$ is light transmittance and $K_{e,\lambda}$ and y are absorption efficiency and material thickness (10 mm glass cuvette), respectively.

2.4. Photo-Thermal Energy Conversion Efficiency of MWCNT Nanofluid

A schematic of the photo-thermal energy conversion experimental device is shown in Figure 5. The nanofluid was filled in a glass-topped beaker that faced the light source. Each beaker had three temperature sensors (top, middle and bottom) connected to the data acquisition system. The photo-thermal energy conversion experimental setup consisted of four main components. The main experimental chamber which contained five glass-topped beakers, the data acquisition system consisted of 16 temperature sensors, one light source radiance meter and a computer. The most important part of this experiment was the light source. In this study, the sun was used as a light source in the test. To prevent any radiation and conduction heat transfer from the outside, aluminum insulation on the outside and foam insulation on the inside were used. The solar weighted absorption fraction is given by Equation (4).

$$A_m = \frac{\int_{\lambda_{\min}}^{\lambda_{\max}} S_m (1 - \mathrm{e}^{k(\lambda)\mathrm{x}}) \mathrm{d}\mathrm{x}}{\int_{\lambda_{\min}}^{\lambda_{\max}} S_m(\lambda) \mathrm{d}\lambda} \tag{4}$$

where, S_m is the solar spectral irradiance in the atmosphere and $K(\lambda)$ is the extinction coefficient by wavelength. The photo-thermal energy conversion efficiency can be expressed by Equation (5).

$$\eta = \frac{mc_p(T_s - T_i)}{GA\Delta t} \tag{5}$$

where, m and c_p are the mass and specific heat of the nanofluid, T_i is initial temperature, T_s is instantaneous temperature, A is the top surface area of the receiver, G is the heat flux of incident solar and Δt is the time of exposed solar radiation.

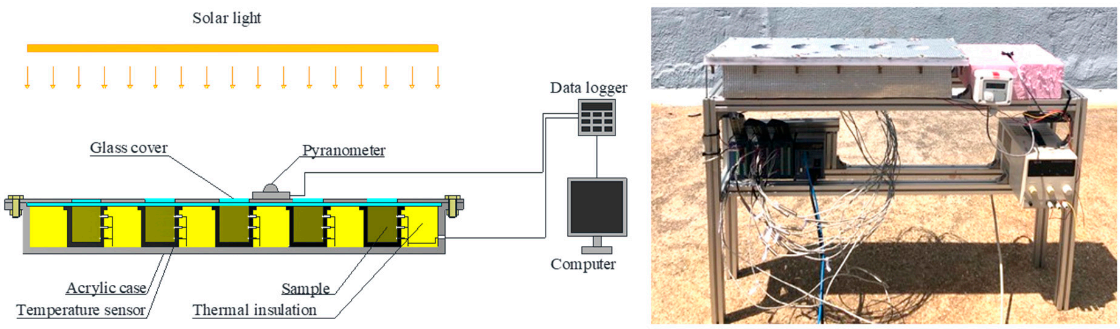

Figure 5. Schematics and picture of photo-thermal energy conversion experimental setup.

Also, according to the Carolina et al. [34] the photo-thermal energy conversion property can be calculated by stored energy ratio (SER) and total stored energy by fluid (E_{total}). The stored energy ratio can calculate the extra energy absorbed by the nanofluid because of the presence of nanoparticles. SER evaluated by the ratio between stored energy of the nanofluid and base fluid. SER of this study can be calculated by Equation (6).

$$\text{SER} = \frac{Q_{nf}(t)}{Q_{bf}(t)} = \frac{(m_{bf}c_{bf} + m_{np}c_{np})(T_{nf}(t) - T_{bf}(0))}{m_{bf}c_{bf}(T_{bf}(t) - T_{bf}(0))} \quad (6)$$

where m_{np} and m_{bf} are mass of nanoparticle and base fluid, c_{np} and c_{bf} represents specific heat capacity of nanoparticle and base fluid, additionally T_{nf} *and* T_{bf} are the temperature of nanofluid and base fluid. In case of $m_{np}c_{np} \ll m_{bf}c_{bf}$, then Equation (6) can be simplified as Equation (7):

$$\text{SER} = \frac{(T_{nf}(t) - T_{bf}(0))}{(T_{bf}(t) - T_{bf}(0))} \quad (7)$$

The total stored energy by fluid can be expressed as Equation (8) [34]:

$$E_{total} = m_f\, c_f\, (T_{max} - T_{min}) \quad (8)$$

T_{max} and T_{min} represents the maximum and minimum temperature of the fluid.

3. Results and Discussion

3.1. Optical Transmittance and Extinction Coefficient of MWCNT Nanofluid

To investigate the optical properties of MWCNT nanofluid, an optical experiment was carried out at room temperature (25 °C) and under the solar wave ranges of 300–1300 nm. Figure 6 shows the variation of the optical transmittance of MWCNT nanofluid according to the concentration. Both MWCNT nanofluid had low transmittance compared with the base fluid (20 vol% ethylene glycol/water). That can be explained by the transparent color of the base fluid because they cannot efficiently absorb the light. The transmittance of the nonfunctionalized MWCNT nanofluid was enhanced by adding the surfactant (gum-arabic) because gum-arabic has a higher transmittance in wavelength ranges of 500–1000 nm compared with the functionalized MWCNT nanofluid [35]. The functionalized MWCNT nanofluid had a higher absorption of solar waves, especially in low light spectrum range (300–700 nm) than the nonfunctionalized MWCNT nanofluid. The functionalized MWCNT nanofluid could completely absorb all of the wavelengths. Moreover, in both MWCNT nanofluid, the transmittance increased as the concentration of the MWCNT nanofluid decreased. In the functionalized MWCNT nanofluid, the transmittance of light was almost zero for the concentration of 0.002 wt%, whereas it was almost zero for the concentration of 0.005wt% nonfunctionalized MWCNT nanofluid. In this optical transmittance experiment, both MWCNT nanofluid had the highest absorption performance at a concentration of 0.01 wt%.

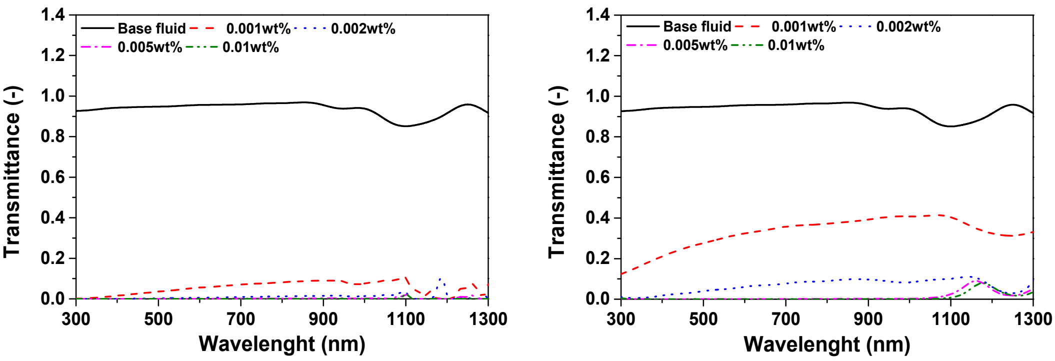

(**a**) Functionalized MWCNT nanofluid (**b**) Nonfunctionalized MWCNT nanofluid

Figure 6. Variation of optical transmittance of (**a**) functionalized and (**b**) nonfunctionalized MWCNT nanofluid.

Figure 7 presents the variation of the extinction coefficient of the functionalized and nonfunctionalized MWCNT nanofluid. In this experiment, it was measured how heavily an MWCNT molecule absorbs the light under a given wavelength range. For both MWCNT nanofluid, the extinction coefficient increased with the increase of concentration of the MWCNT nanofluid. A high extinction coefficient in a wavelength ranges of 300–900 nm was found in both the functionalized and nonfunctionalized MWCNT nanofluid. In addition, the extinction coefficient gradually decreased under long-wavelength ranges. As the wavelength increased, the extinction coefficient of the functionalized MWCNT nanofluid decreased compared with the nonfunctionalized one. Additionally, at a concentration of 0.01 wt%, both MWCNT nanofluid exhibited an unstable trend in the extinction coefficient because of the small amount of agglomeration of nanoparticles under high concentration.

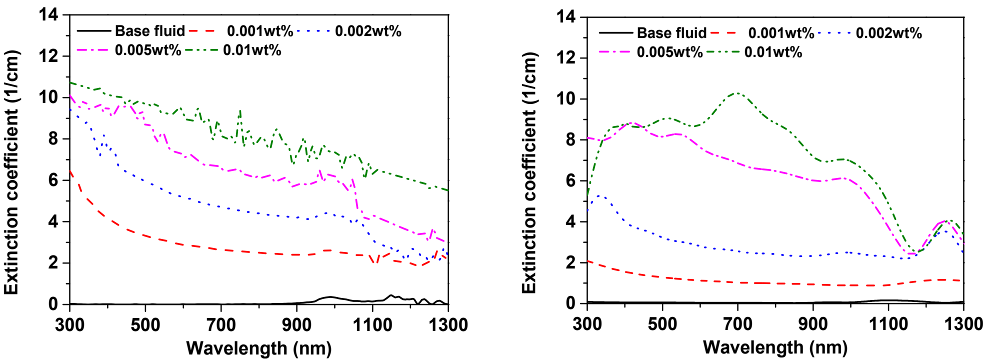

(**a**) Functionalized MWCNT nanofluid (**b**) Nonfunctionalized MWCNT nanofluid

Figure 7. Extinction coefficient of (**a**) functionalized and (**b**) nonfunctionalized MWCNT nanofluid.

Figure 8 shows the variation of the solar weighted absorption fraction of the MWCNT nanofluid. In Figure 8b, the solar weighted absorption fraction of the nonfunctionalized MWCNT nanofluid at a short penetration distance was different according to the concentration of the nanofluid. Additionally, the solar weighted absorption fraction reached the maximum value separately according to the concentration. The solar weighted absorption fraction of the nonfunctionalized MWCNT nanofluid was 1.0 at a penetration distance of 5 cm for all concentrations, especially at concentrations of 0.001 and 0.002 wt%. At a concentration of 0.005 wt%, it was 1.0 at a penetration distance of 1 cm. In the case of the functionalized MWCNT nanofluid, the solar weighted absorption fraction was not significantly influenced by the concentration of nanofluid. In the functionalized MWCNT nanofluid, the solar weighted absorption fraction was 1 at a penetration distance of 1 cm except for 0.001 wt%. In the case of 0.001wt% functionalized MWCNT nanofluid, it was 2 cm to reach the maximum solar weighted absorption fraction (1.0). The base fluid absorbed only 27.1% of solar energy at a penetration distance of 5 cm and the percentage increased as the penetration distance increased. The lowest solar weighted absorption fraction was observed at a MWCNT nanofluid concentration of 0.001 wt%. Additionally, functionalized MWCNT nanofluid almost absorbed all solar energy at all concentrations compared with the nonfunctionalized one. It can be inferred that the functionalization of MWCNT nanoparticles can improve the solar absorption characteristics of the MWCNT nanofluid.

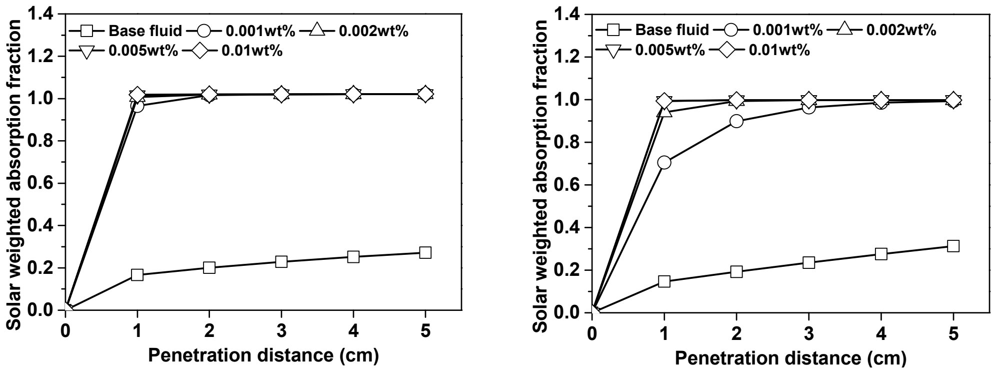

(**a**) Functionalized MWCNT nanofluid (**b**) Nonfunctionalized MWCNT nanofluid

Figure 8. Solar weighted absorption fraction of (**a**) functionalized and (**b**) nonfunctionalized MWCNT nanofluid.

3.2. Thermal Conductivity Characteristics of MWCNT Nanofluid

The variation of the thermal conductivity of functionalized and nonfunctionalized MWCNT nanofluid is presented in Figure 9. The thermal conductivity of the MWCNT nanofluid increased with the increase of temperature. Furthermore, adding MWCNT nanoparticles into the base fluid can increase thermal conductivity significantly. In the case of the base fluid, the thermal conductivities of the ethylene glycol/water solution were 0.49 and 0.522 W/m°C at temperatures of 20 °C and 50 °C, that fits the ASHRAE [32] and Harkireat [36] results, respectively. Compared with the base fluid, the maximum increase of thermal conductivity was 10.15%, which was observed at a temperature of 50°C and a functionalized MWCNT nanofluid concentration of 0.01 wt%. The thermal conductivities of the functionalized and nonfunctionalized MWCNT nanofluid were 0.511 W/m°C and 0.502 W/m°C at 20 °C and 0.54 W/m°C and 0.538 W/m°C at 50 °C, respectively, when the concentration MWCNT nanofluid was 0.01 wt%. Compared with the base fluid, 4.23% and 2.5% enhancements in thermal conductivity were observed in functionalized and nonfunctionalized MWCNT nanofluid at a concentration and temperature of 0.01 wt% and 20 °C and 10.15% and 9.93% enhancement in thermal conductivity was shown at 0.01 wt% and 50 °C, respectively. Figure 9a,b show the similar increment trend of thermal conductivity for two kinds of MWCNT nanofluid.

In Figure 9b, the experimental result revealed that the thermal conductivity of nonfunctionalized MWCNT nanofluid significantly increased with rising temperature and concentration of the nanofluid. Both figures show that there is a parallel tendency for concentrations and temperature. Additionally, the tendency of both graphs is almost similar to that in previous studies on the thermal conductivity of nanofluid [37–44]. The temperature effect on the improvement of thermal conductivity in nanofluid is mainly caused by the increase in the intensity of Brownian motion that is the result of augmentation of interactions and movement between nanoparticles. Furthermore, this study confirmed that the effect of concentration on the thermal conductivity enhancement is surprisingly superior at higher temperatures. In both MWCNT nanofluid, the increment of thermal conductivity at a lower temperature range was more rapid than at a higher temperature range. In other words, the functionalized and nonfunctionalized MWCNT nanofluid exhibited logarithmic variation of thermal conductivity enhancement, as shown in Figure 9.

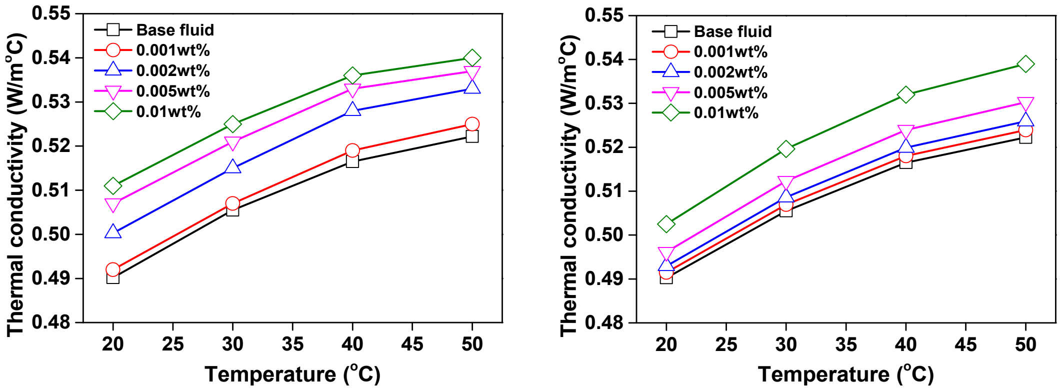

(**a**) Functionalized MWCNT nanofluid (**b**) Nonfunctionalized MWCNT nanofluid

Figure 9. Variation of thermal conductivity with temperature at different weight concentrations of (**a**) functionalized and (**b**) nonfunctionalized MWCNT nanofluid.

Figure 10 shows the variation of thermal conductivity according to the concentration of functionalized and nonfunctionalized MWCNT nanofluid. Thermal conductivity increased with the increase of concentration of MWCNT nanofluid. Compared with the functionalized MWCNT nanofluid, the increase of thermal conductivity of nonfunctionalized MWCNT nanofluid was more linear. For the concentration of 0.001 wt%, the functionalized MWCNT nanofluid demonstrated exponential line; thus, it can be assumed that when the concentration increases beyond the critical concentration, the thermal conductivity may not increase anymore, as shown in Figure 10a. In Figure 9, in the case of the nonfunctionalized MWCNT nanofluid, gaps between concentration curves increased with an increase of concentration. However, in the case of the functionalized MWCNT nanofluid, the opposite phenomenon was observed. The gap between concentration curves in the functionalized MWCNT nanofluid decreased with the increase of concentration. As the concentration of MWCNT nanofluid increased from 0.001 to 0.002wt%, the enhancements of thermal conductivity of functionalized and nonfunctionalized MWCNT nanofluid were 1.68% and 0.29% at 20 °C and 1.52% and 0.38% at 50 °C, respectively. In addition, they were 0.78% and 1.28% at 20 °C and 0.18% and 1.63% at 50 °C, respectively, when the concentration of the MWCNT nanofluid increased from 0.005 to 0.01 wt%. It can be inferred that the reason for the decrement of thermal conductivity enhancement was the side effect of MWCNT functionalization. In the case of the functionalized MWCNT nanofluid, a high concentration could cause little agglomeration in the MWCNT nanofluid, which also can be explained by the enhancement reduction of thermal conductivity.

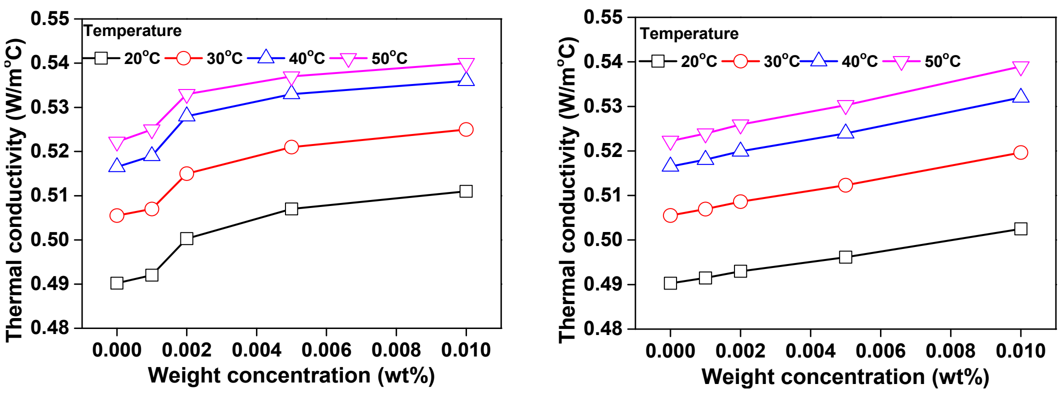

(**a**) Functionalized MWCNT nanofluid (**b**) Nonfunctionalized MWCNT nanofluid

Figure 10. Thermal conductivity of the (**a**) functionalized and (**b**) nonfunctionalized MWCNT nanofluid with weight concentration for different temperatures.

3.3. Photo-Thermal Energy Conversion Characteristics of MWCNT Nanofluid

Figure 11 shows the temperature variation of functionalized and nonfunctionalized MWCNT nanofluid according to the time during the photo-thermal energy conversion experiment. All MWCNT nanofluid were heated by the unstable actual solar with average solar irradiation of 800 W/m^2 for more than 2 h. The temperature of the MWCNT nanofluid increased as the operating time passed. For both MWCNT nanofluid, the photo-thermal energy conversion ability increased disproportionately with an increase of concentration, which can be also explained by the enhancement of thermal conductivity. That means that the increase of thermal conductivity of the MWCNT nanofluid can bring the enhancement of convection heat transfer and specific heat in the working fluid. The functionalized MWCNT nanofluid had a better ability to store and convert solar thermal energy because of its high specific heat compared with the nonfunctionalized MWCNT nanofluid. Moreover, the temperature of the functionalized MWCNT nanofluid increased faster than that of the nonfunctionalized MWCNT nanofluid and base fluid. The maximum temperature increment was 8.6 °C and it was observed in the functionalized MWCNT nanofluid at a concentration of 0.005 wt%. In the case of the base fluid, the temperature increased by 5.2 °C after 2 h. The temperature of the functionalized and nonfunctionalized MWCNT nanofluid increased by 7.9 °C and 7.5 °C at a concentration of 0.002 wt% and it also increased by 8.6 °C and 8.2 °C at a concentration of 0.005 wt%, respectively. In Figure 11, the unstable temperature increment of MWCNT nanofluid is shown. It was mostly caused by inconsistent solar radiation from the sun. The ability of photo-thermal energy conversion can be enhanced by adding a small amount of MWCNT nanoparticles into the base fluid. Additionally, it can be inferred that the functionalization of MWCNT nanoparticles can bring an improvement of the photo-thermal energy conversion capability.

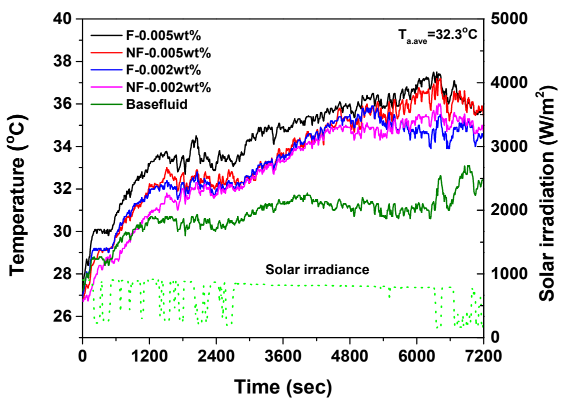

Figure 11. Variation of temperature with time for functionalized and nonfunctionalized MWCNT nanofluid.

Figure 12 presents the SER for the functionalized and nonfunctionalized MWCNT nanofluid for the different weight concentrations. The SER (stored energy ratio) increased in case of addition of MWCNT nanoparticles into the EG (20 wt%). As a result, the F-0.005 wt% nanofluid presents the maximum SER, while NF-0.002 wt% nanofluid shows the minimum SER. The maximum SER was 2.78 which was observed at a concentration of 0.005wt% functionalized MWCNT after 6000 sec. In addition, the functionalization of MWCNT nanoparticle can enhance SER of nanofluid under wide operating conditions. The difference between the maximum and minimum SER lines are greater at first 1200 sec than the last period of experimental time, which indicates the concentration effect was stronger in the first 20 min compared to the last period of operating time. The concentration effect on SER was dominant at first 2400 sec because the temperature increment of nanofluid was higher in the first period of the experiment. After a first half of operating time in the photo-thermal energy conversion experiment, SER was increased significantly again due to the increase of ambient temperature.

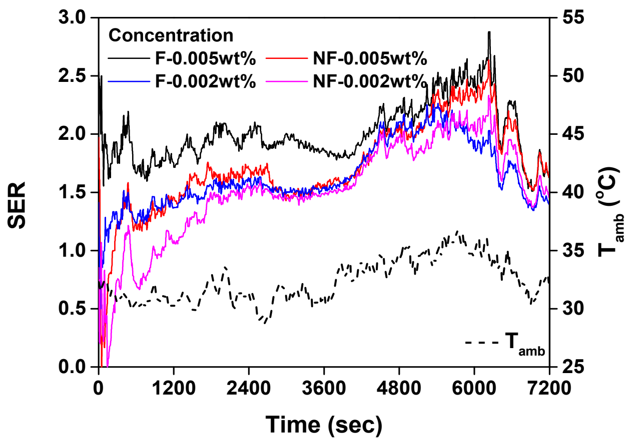

Figure 12. Stored Energy Ratio (SER) for functionalized and nonfunctionalized MWCNT nanofluid.

To investigate the photo-thermal energy conversion performance of the MWCNT nanofluid in more detail, three thermocouples at three points (top, bottom and middle) in each sample beaker were used in the photo-thermal energy conversion experiment. Figure 13 shows the temperature increase of the MWCNT nanofluid according to the sensor location after 2 h. Compared with the base fluid, the functionalized and nonfunctionalized MWCNT nanofluid showed a lower temperature at the bottom sensor because of low light transmittance. The top temperatures of the functionalized and nonfunctionalized MWCNT nanofluid were 8.2 °C and 8.1 °C at a concentration of 0.005 wt% and they also were 7.9 °C and 7.5 °C at a concentration of 0.002 wt%, respectively. However, the top temperature of the base fluid was 5.2 °C. Furthermore, the functionalized and nonfunctionalized MWCNT nanofluid show high temperature in the top sensor because of the high solar energy absorption fraction in the top part. The bottom temperatures of the functionalized and nonfunctionalized MWCNT nanofluid were 5 °C and 5.2 °C at a concentration of 0.005 wt% and they also were 5.3 °C and 5.3 °C at a concentration of 0.002 wt%, respectively. However, the bottom temperature of the base fluid was 6.6 °C. The bottom temperature of the MWCNT nanofluid decreased as the concentration increased, which indicated that the light could not pass through the whole MWCNT nanofluid to the bottom because of low light transmittance. In addition, most of the solar energy was almost absorbed in the MWCNT nanofluid at the top area owing to superior solar absorption characteristics. However, the opposite trend was shown in the base fluid. Because the base fluid does not have good absorption performance, most of the solar radiation can reach the bottom area through the test section. Therefore, the temperature of the base fluid at the bottom was the highest.

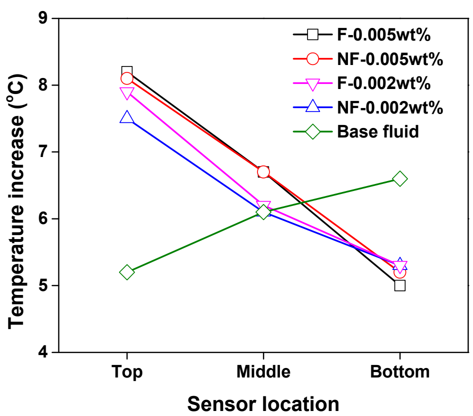

Figure 13. Variation of temperature increase of MWCNT nanofluid according to sensor location.

Figure 14 shows the total stored energy during the heating process in function of the weight concentration of functionalized and nonfunctionalized MWCNT nanofluid. The result indicates that the addition of MWCNT nanoparticles into base fluid can increase in the total stored energy significantly. The maximum total stored energy was presented at the F-0.005 wt% nanofluid but the difference of total stored energy between the functionalized and nonfunctionalized MWCNT nanofluid with the concentration of 0.002 wt% and 0.005 wt% was very small, it is just about 2% and 1%, respectively. The concentration effect on the increase of total stored energy was greater than the functionalization effect of MWCNT nanofluid. Compared to the base fluid, the maximum enhancement of total stored energy was 77.6% at the F-0.005 wt% MWCNT nanofluid.

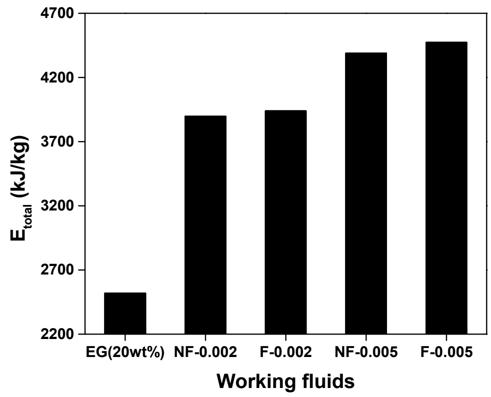

Figure 14. Total stored energy during heating process in function of the weight concentration of functionalized and nonfunctionalized MWCNT nanofluid.

Figure 15 presents the photo-thermal energy conversion efficiency for different MWCNT nanofluid according to time. The photo-thermal energy conversion efficiency of MWCNT nanofluid decreased with the operating time and increased with the concentration of nanofluid. Moreover, the functionalization of the MWCNT nanofluid had better photo-thermal energy conversion efficiency than the nonfunctionalized one, which can be described by the increase of the specific heat and thermal conductivity of the nanofluid. The photo-thermal energy conversion efficiencies of functionalized and nonfunctionalized MWCNT nanofluid decreased from 60% to 19.1% and from 57% to 18.6% at concentrations of 0.005 wt% after 2 h, respectively. When the temperature of the working fluid increased, the heat loss from the working fluid to ambient was also increased. This can explain the decrease of the photo-thermal energy conversion efficiency as time passed. With the addition of MWCNT nanoparticles into the base fluid, the photo-thermal energy conversion efficiency increased significantly because of the good thermal properties and other positive effects. In addition, at the same concentration, the functionalized MWCNT nanofluid could reach a higher temperature under the same solar radiation than the nonfunctionalized one. Therefore, the functionalized MWCNT nanofluid has better solar light absorption capability than the nonfunctionalized MWCNT nanofluid and water.

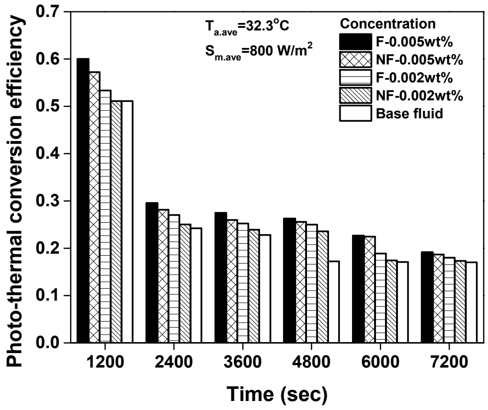

Figure 15. Comparison of photo-thermal energy conversion efficiency for different MWCNT nanofluid with time.

4. Conclusions

In this study, the thermal conductivity, optical transmittance and photo-thermal energy conversion efficiency of two different types of MWCNT nanofluid were compared experimentally. As a result, the functionalized MWCNT nanofluid has a higher thermal conductivity and dispersion stability than those of the nonfunctionalized MWCNT nanofluid. The maximum increase of thermal conductivity was 10.15% at a temperature of 50 °C and the concentration of 0.01 wt% in the functionalized MWCNT nanofluid. The thermal conductivities of the functionalized and nonfunctionalized MWCNT nanofluid were 0.511 W/m°C and 0.502 W/m°C at 20 °C and 0.54 W/m°C and 0.538 W/m°C at 50 °C in a concentration of 0.01wt%, respectively. Compared with the base fluid, in the case of a concentration of 0.01 wt%, 4.23% and 2.5% enhancements in thermal conductivity were observed in the functionalized and nonfunctionalized MWCNT nanofluid at a temperature of 20 °C and 10.15% and 9.93% enhancements were also measured at a temperature of 50 °C, respectively.

According to the optical experimental result, light absorption increased with nanofluid concentration. In the case of the functionalized MWCNT nanofluid, the solar weighted absorption fraction was not influenced seriously by the concentration of nanofluid. The functionalized MWCNT nanofluid had a better solar light absorption capability compared with that of the nonfunctionalized one and water. The photo-thermal energy conversion efficiency of the MWCNT nanofluid decreased with the operating time and increased with the concentration of nanofluid. Moreover, the functionalized MWCNT nanofluid has better photo-thermal energy conversion efficiency than the nonfunctionalized MWCNT nanofluid. The photo-thermal energy conversion efficiencies of the functionalized and nonfunctionalized MWCNT nanofluid decreased from 60% to 19.1% and from 57% to 18.6% at a concentration of 0.005 wt% after 2 h, respectively. Consequently, adding functionalized MWCNT nanofluid in a thermal system can lead to the enhancement of thermal efficiency and possibly reduce the size of a heat exchanger.

Author Contributions: Conceptualization, H.C. and T.B.; methodology J.H.; validation, H.C., T.B. and J.H.; formal analysis, J.H.; investigation, T.B.; resources, H.C.; writing—original draft preparation, T.B.; writing—review and editing, H.C. and J.H.; visualization, T.B.; supervision, H.C.

Acknowledgments: This research was supported by the Basic Science Research Program through the National Research Foundation of Korea (NRF) funded by the Ministry of Science, ICT & Future Planning (NRF-2017R1A2B4006125) and Human Resources Program in Energy Technology of the Korea Institute of Energy Technology Evaluation and Planning (KETEP), granted financial resources from the Ministry of Trade, Industry & Energy, Republic of Korea (No. 20194030202410).

Conflicts of Interest: The authors declare no conflict of interest. The funders had no role in the design of the study; in the collection, analyses, or interpretation of data; in the writing of the manuscript, or in the decision to publish the results.

References

1. Global Energy Statistical Yearbook 2019. Available online: www.yearbook.enerdata.net (accessed on 27 August 2019).
2. Choi, S.U.S.; Eastman, J.A. Enhancing thermal conductivity of fluids with nanoparticles. In *International Mechanical Engineering Congress and Exhibition*; Argonne National Lab: San Francisco, CA, USA, 1995; pp. 12–17.
3. Guo, W.; Li, G.; Zheng, Y.; Dong, C. Measurement of the thermal conductivity of SiO_2 nanofluid with an optimized transient hot wire method. *Thermochim. Acta* **2018**, *661*, 84–97. [CrossRef]
4. Kumar, N.; Sonawane, S.S. Experimental study of thermal conductivity and convective heat transfer enhancement using CuO and TiO_2 nanoparticles. *Int. Commun. Heat Mass Transf.* **2016**, *76*, 98–107. [CrossRef]
5. Wei, B.; Zou, X.; Li, X. Experimental investigation on stability and thermal conductivity of diathermic oil based TiO_2 nanofluid. *Int. Heat Mass Transf.* **2017**, *104*, 537–543. [CrossRef]
6. Vakili, M.; Karami, M.; Delfani, S.; Khosrojerdi, S.; Kalhor, K. Experimental investigation and modeling of thermal conductivity of CuO–water/EG nanofluid by FFBP-ANN and multiple regressions. *Therm. Anal. Calorim.* **2017**, *129*, 629–637. [CrossRef]
7. Ahmadi, M.H.; Mirlohi, A.; Nazari, M.A.; Roghayeh, G. A review of thermal conductivity of various nanofluid. *Mol. Liq.* **2018**, *265*, 181–188. [CrossRef]
8. Pryazhnikov, M.I.; Minakov, A.V.; Rudyak, V.Ya.; Guzei, D.; Guzei, D.V. Thermal conductivity measurements of nanofluid. *Heat Mass Transf.* **2017**, *104*, 1275–1282. [CrossRef]
9. Kim, H.; Kim, J.; Cho, H. Review of Thermal Performance and Efficiency in Evacuated Tube Solar Collector with Various Nanofluid. *Int. Air-Cond. Refrig.* **2017**, *25*, 1730001. [CrossRef]
10. Kang, W.; Shin, Y.; Cho, H. Economic Analysis of Flat-Plate and U-Tube Solar Collectors Using an Al_2O_3 Nanofluid. *Energies* **2017**, *10*, 1911. [CrossRef]
11. Lee, J.H.; Hwang, S.G.; Lee, G.H. Efficiency Improvement of a Photovoltaic Thermal (PVT) System Using Nanofluids. *Energies* **2019**, *12*, 3063. [CrossRef]
12. Sarafraz, M.M.; Safei, M.R.; Leon, A.S.; Tlili, I.; Alkanhal, A.; Tian, Z.; Goodarzi, M.; Arjomandi, M. Experimental Investigation on Thermal Performance of PV/T-PCM (Photovoltaic/Thermal) System Cooling with a PCM and Nanofluid. *Energies* **2019**, *13*, 2572. [CrossRef]
13. Bergman, T.L.; Lavine, A.S. Appendix. In *Incropera's Principle of Heat and Mass Transfer*; John Wiley & Sons Inc.: New York, NY, USA, 1981; pp. 914–916.
14. Gan, Y.; Qiao, L. Optical Properties and Radiation-Enhanced Evaporation of Nanofluid Fuels Containing Carbon-Based Nanostructures. *Energy Fuels* **2012**, *26*, 4224–4230. [CrossRef]
15. Meng, Z.; Wu, D.; Wang, L.; Zhu, H.; Li, Q. Carbon nanotube glycol nanofluid: Photo-thermal properties, thermal conductivities and rheological behavior. *Particuology* **2012**, *10*, 614–618. [CrossRef]
16. Zeiny, A.; Jin, H.; Bai, L.; Lin, G.; Wen, D. A comparative study of direct absorption nanofluid for solar thermal application. *Sol. Energy* **2018**, *161*, 74–82. [CrossRef]
17. Kumar, D.D.; Arasu, A.V. A comprehensive review of preparation, characterization, properties and stability of hybrid nanofluid. *Renew. Sustain. Energy Rev.* **2018**, *81*, 1669–1689. [CrossRef]
18. Sidik, N.A.C.; Jamil, M.M.; Japar, W.M.A.; Adamu, I.M. A review on preparation methods, stability and applications of hybrid nanofluid. *Renew. Sustain. Energy Rev.* **2017**, *80*, 1112–1122. [CrossRef]
19. Barnali, M.; Nareshbabu, K.; Shampa, R.S.; Pradeepkumar, J.; Jibao, H.; Ramamurthy, V. Synthesis, Characterization, Guest Inclusion, and Photophysical Studies of Gold Nanoparticles Stabilized with Carboxylic Acid Groups of Organic Cavitands. *Langmuir* **2013**, *29*, 12703–12709.
20. Yazid, M.; Nor, A.C.S.; Mamat, R.; Najafi, G. A review of the impact of preparation on stability of carbon nanotube nanofluid. *Int. Commun. Heat Mass* **2019**, *78*, 253–263. [CrossRef]
21. Farbod, M.; Ahangarpour, S.; Etemad, G. Stability and thermal conductivity of water-based carbon nanotube nanofluid. *Particuology* **2015**, *22*, 59–65. [CrossRef]
22. Karami, M.; Akhavan, B.M.A.; Delfani, S.; Ghozatloo, A. A new application of carbon nanotubes nanofluid as working fluid of low-temperature direct absorption solar collector. *Sol. Energy Mater. Sol. Cells* **2014**, *121*, 114–118. [CrossRef]
23. Mesgari, S.; Taylor, R.A.; Hjerrild, N.E.; Felipre, C.; Li, Q.; Jason, S. An investigation of thermal stability of carbon nanofluid for solar thermal applications. *Sol. Energy Mater. Sol. Cells* **2016**, *157*, 652–659. [CrossRef]

24. Hewakuruppu, Y.L.; Taylor, R.A.; Tyagi, H.; Khullar, V.; Otanicar, T.; Sylvain, C.; Nathan, H. Limits of selectivity of direct volumetric solar absorption. *Sol. Energy* **2015**, *114*, 206–216. [CrossRef]
25. Shende, R.C.; Ramaprabhu, S. Thermo-optical properties of partially unzipped multiwalled carbon nanotubes dispersed nanofluid for direct absorption solar thermal energy systems. *Sol. Energy Mater. Sol. Cells* **2016**, *157*, 117–125. [CrossRef]
26. Soltanimehr, M.; Afrand, M. Thermal conductivity enhancement of COOH-functionalized MWCNT/ethylene glycol-water nanofluid for application in heating and cooling application. *Appl. Therm. Eng.* **2016**, *105*, 716–726. [CrossRef]
27. Jian, Q.; Tian, M.; Han, X.; Zhang, R.; Wang, Q. Photo-thermal conversion characteristics of MWCNT-H_2O nanofluid for direct solar thermal energy absorption application. *Appl. Therm. Eng.* **2017**, *124*, 486–493.
28. Zeng, J.; Xuan, Y. Enhanced solar thermal conversion and thermal conduction of MWCNT-SiO_2/Ag binary nanofluid. *Appl. Energy* **2018**, *212*, 809–819. [CrossRef]
29. Nadooshan, A.A.; Eshgari, H.; Afrand, M. Measuring viscosity of Fe_3O_4-MWCNT/EG hybrid nanofluid for evaluation of thermal efficiency: Newtonian and non-Newtonian behavior. *Mol. Liq.* **2018**, *253*, 169–177. [CrossRef]
30. Ham, J.; Shin, Y.; Cho, H. Optical-thermal properties of an MWCNT/EG nanofluid intended as the working fluid in a direct absorption solar collector. *High Temp-High Press* **2019**, *48*, 121–139. [CrossRef]
31. Sundar, L.S.; Singh, M.K.; Antonio, C.M.S. Enhanced heat transfer and friction factor of MWCNT–Fe_3O_4/water hybrid nanofluid. *Int. Commun. Heat Mass* **2014**, *52*, 73–83. [CrossRef]
32. Claridge, D.E.; Frederick, H.K.; Brian, A.R.; Underwood, T.D.; Micheal, W.W. *American Society of Heating, Refrigerating and Air-Conditioning Engineers*; ASHRAE: Atlanta, GA, USA, 2001; pp. 427–428.
33. Howell, J.R.; Siegel, R.; Menguc, M.P. Thermal Radiation Heat Transfer. In *National Aeronautics and Space Administration*, 5th ed.; CRC Press: Boca Raton, FL, USA, 2011.
34. Carolina, L.L.B.; Amjad, M.; Filho, P.E.B.; Wen, D. Experimental study of photothermal conversion using gold/water and MWCNT/water nanofluid. *Sol. Energy Mater. Sol. Cells* **2018**, *188*, 51–65.
35. Adam, H.; Sidding, M.A.; Sidding, A.A.; Eltahir, N.A. Electrical and optical properties of two types of Gum Arabic. *Sudan Med. Monital.* **2013**, *8*, 174–178.
36. Harkireat, S.; Gangacharyulu, D. An experimental study on stability and some thermophysical properties of multiwalled carbon nanotubes with water–ethylene glycol mixtures. *Particul. Sci. Technol.* **2017**, *35*, 547–554.
37. Esfahani, M.R.; Languri, E.M.; Nunna, M.R. Effect of particle size and viscosity on thermal conductivity enhancement of graphene oxide nanofluid. *Int. Commun. Heat Mass* **2016**, *76*, 308–315. [CrossRef]
38. Chai, Y.H.; Yusup, S.; Chok, V.S.; Arpin, M.T.; Irawan, S. Investigation of thermal conductivity of multi walled carbon nanotube dispersed in hydrogenated oil based drilling fluids. *Appl. Therm. Eng.* **2016**, *107*, 1019–1025. [CrossRef]
39. Shamaeil, M.; Firouzi, M.; Fakhar, A. The effects of temperature and volume fraction on the thermal conductivity of functionalized DWCNTs/ethylene glycol nanofluid. *Therm. Anal. Calorim.* **2016**, *126*, 1455–1462. [CrossRef]
40. Xing, M.; Yu, J.; Wang, R. Experimental investigation and modelling on the thermal conductivity of CNTs based nanofluid. *Int. Therm. Sci.* **2016**, *104*, 404–411. [CrossRef]
41. Esfea, M.H.; Esfandeh, S.; Saedodinn, S.; Rostamian, H. Experimental evaluation, sensitivity analyzation and ANN modeling of thermal conductivity of ZnO-MWCNT/EG-water hybrid nanofluid for engineering applications. *Appl. Therm. Eng.* **2017**, *125*, 673–685. [CrossRef]
42. Harandi, S.S.; Karimipour, A.; Afrand, M.; Akbari, M.; D'Orazio, A. An experimental study on thermal conductivity of F-MWCNTs–Fe_3O_4/EG hybrid nanofluid: Effects of temperature and concentration. *Int. Commun.* **2016**, *76*, 171–177.
43. Bhattad, A.; Sarkar, J.; Ghosh, P. Energy-Economic Analysis of Plate Evaporator using Brine-based Hybrid Nanofluid as Secondary Refrigerant. *Int. I. Air-Cond. Refrig.* **2018**, *26*, 1850003. [CrossRef]
44. Kim, M.B.; Park, H.G.; Park, C.Y. Change of Thermal Conductivity and Cooling Performance for Water Based Al_2O_3-Surfactant Nanofluid with Time Lapse. *Int. I. Air-Cond. Refrig.* **2018**, *26*, 1850009. [CrossRef]